Available online at www.sciencedirect.com

SCIENCE DIRECT®

ELSEVIER

International Journal of Heat and Mass Transfer 48 (2005) 3119–3127

International Journal of HEAT and MASS TRANSFER

www.elsevier.com/locate/ijhmt

Constructal design of forced convection cooled microchannel heat sinks and heat exchangers

Y.S. Muzychka

Faculty of Engineering and Applied Science, Memorial University of Newfoundland, St. John's, NF, Canada A1B 3X5

Received 30 December 2004; received in revised form 4 February 2005
Available online 12 April 2005

Abstract

Heat transfer from arrays of circular and non-circular ducts subject to finite volume and constant pressure drop constraints is examined. It is shown that the optimal duct dimension is independent of the array structure and hence represents an optimal construction element. Solutions are presented for the optimal duct dimensions and maximum heat transfer per unit volume for the parallel plate channel, rectangular channel, elliptic duct, circular duct, polygonal ducts, and triangular ducts. Approximate analytical results show that the optimal shape is the isosceles right triangle and square duct due to their ability to provide the most efficient packing in a fixed volume. Whereas a more exact analysis reveals that the parallel plate channel array is in fact the superior system. An approximate relationship is developed which is very nearly a universal solution for any duct shape in terms of the Bejan number and duct aspect ratio. Finally, validation of the relationships is provided using exact results from the open literature.

Keywords: Constructal design; Microchannels; Non-circular ducts; Internal structure; Forced convection; Laminar flow; Optimal geometry

1. Introduction

Microchannels are at the fore front of today's cooling technologies. They are widely being considered for cooling of electronic devices and in microheat exchanger systems due to their ease of manufacture. On a larger scale, compact heat exchangers also frequently utilize small passage geometries having characteristic length scales less than 3 mm. One issue which arises in the use of microchannels is related to the small length scale of the channel or duct cross-section. That is, as the characteristic length scale of the cross-section becomes smaller and smaller, the propensity for fully developed laminar flow increases. Since heat transfer coefficient diminishes with increasing flow length as does the heat transfer effectiveness of the fluid, it is desirable to maximize heat transfer for a fixed volume and mean system temperature. This issue can be addressed by considering the elemental passage geometries and determining the best passage size and configuration for a fixed volume, which is to be convectively cooled with a fluid stream supplied at constant pressure drop.

Bejan and Sciubba [1] first considered this problem for an array of parallel plates with application to the cooling of electronic systems. Using the intersection of asymptotes method, Bejan and Sciubba [1] obtained expressions for the optimal plate spacing to channel

E-mail address: yuri@engr.mun.ca

0017-9310/$ - see front matter © 2005 Elsevier Ltd. All rights reserved.
doi:10.1016/j.ijheatmasstransfer.2005.02.014

Nomenclature

A	flow area, m^2
a, b	major and minor axes of ellipse or rectangle, m
Be	Bejan number, $\equiv \Delta p L^2/\mu\alpha$
C_1, C_2, C_3	constants
C_p	specific heat, J/kg K
d	diameter of circular duct, m
D_h	hydraulic diameter, $\equiv 4A/P$
$\mathbf{E}(\cdot)$	complete elliptic integral of second kind
f	friction factor $\equiv \tau/(\frac{1}{2}\rho U^2)$
k	thermal conductivity, W/mK
H	height, m
ℓ	reference length scale, m
L	duct length, m
$\mathscr{L}$	arbitrary length scale, m
n	number of sides of polygon
N	number of channels or ducts
P	perimeter, m
p	pressure, N/m^2
Po	Poiseuille number, $\equiv \bar{\tau}\mathscr{L}/\mu\overline{U}$
Pr	Prandtl number, $\equiv \nu/\alpha$
Q	heat transfer rate, W
$\mathscr{Q}$	heat transfer per unit volume, $\equiv Q/HWL$
$Q^\star$	dimensionless $\mathscr{Q}$, $\equiv \mathscr{Q}L^2/k(\overline{T}_s - T_i)$
r	radius, m
$Re_{\mathscr{L}}$	Reynolds number, $\equiv U\mathscr{L}/\nu$
$\overline{T}_s$	wall or surface temperature, K
T_i	fluid inlet temperature, K
$\overline{U}$	average velocity, m/s
U_∞	free stream velocity, m/s
W	width, m

Greek symbols

α	thermal diffusivity, m^2/s
ϵ	aspect ratio, $\equiv b/a$
μ	dynamic viscosity, $N\,s/m^2$
ν	kinematic viscosity, m^2/s
ρ	fluid density, kg/m^3
τ	wall shear stress, N/m^2

Subscripts

$\sqrt{A}$	based upon the square root of flow area
c	circumscribed
D_h	based upon the hydraulic diameter
f	fluid
i	inscribed
l	large
$\mathscr{L}$	based upon the arbitrary length $\mathscr{L}$
s	small

length ratio, b_{opt}/L, and the maximum heat transfer per unit volume in terms of a dimensionless parameter which is now referred to as the Bejan number [2,3].

Yilmaz et al. [4] applied an exact method of analysis to obtain results for a single duct for the equilateral triangle, square, circular, and parallel plate geometries. The method of analysis is quite involved due the use of of complex generalized empirical correlations developed by one of the authors [4]. The authors [4] also proposed an empirically based formula for the optimal duct shape for these configurations. Fisher and Torrance [5] considered similar problems with conduction effects in the solid array. Finally, Favre-Marinet et al. [6] conducted experiments on microchannels to provide experimental evidence supporting the results reported in Bejan and Sciubba [1].

In the present work, the approximate analysis method of Bejan and Sciubba [1] is applied to several other channel shapes to determine the optimal passage size to length ratio in terms of the Bejan number. It will be shown that these optimal dimensions are independent of the array configuration and thus represent a basic constructional unit for built up systems. These optimal scales are then applied to arrays of passages to determine the maximum heat transfer rate per unit volume. Depending upon the passage shape, several potential packing arrangements can be chosen, each with its own characteristic performance. Results for individual shapes are compared with those reported in Yilmaz et al. [4].

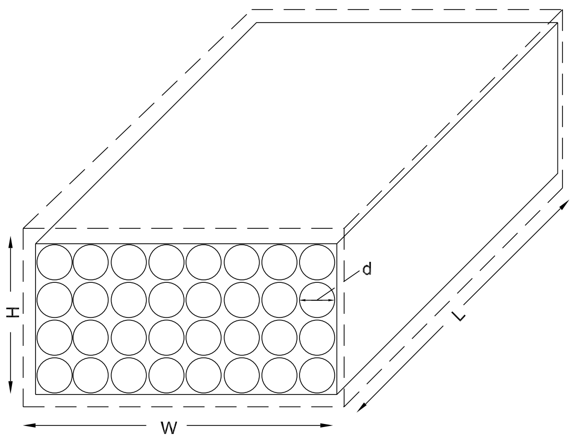

Fig. 1. Convectively cooled finite volume.

2. Hydrodynamic and thermal analysis

The system under consideration consists of a fixed volume to be cooled by means of laminar forced convection. The volume also contains an array of circular or non-circular passages, as shown in Fig. 1. These passages may be arranged in such a manner that their number is maximized. Of particular interest are passages which are rectangular, elliptical, polygonal, or triangular.

The following assumptions are made throughout the analysis: the duct walls are isothermal (negligible conduction resistance in the array), uniform flow distribution (equal flow in all ducts or channels), laminar flow, constant cross-sectional duct area, no inlet or exit plenum losses, Prandtl number range $Pr > 0.1$, and a finite control volume ($V = HWL$).

2.1. Small ducts or channels

In the case of an array of ducts or channels with small cross-sectional characteristic reference length scale, the enthalpy balance for fully developed flow gives

$$Q_s = \rho \overline{U} NAC_p(\overline{T}_s - T_i) \tag{1}$$

where A is the cross-sectional area of an elemental duct or channel, N is the total number of ducts or channels, $\overline{T}_s$ is the mean wall temperature, and T_i is the fluid inlet temperature.

The mean velocity, $\overline{U}$, in any one duct or channel assuming uniform flow distribution, may be determined from the fully developed flow Poiseuille number defined as

$$Po_{\mathscr{L}} = \frac{\overline{\tau}_w \mathscr{L}}{\mu \overline{U}} = \frac{(A/P)(\Delta p/L)\mathscr{L}}{\mu \overline{U}} \tag{2}$$

or

$$\overline{U} = \frac{A\Delta p \mathscr{L}}{\mu PLPo_{\mathscr{L}}} \tag{3}$$

where $\mathscr{L}$ is the characteristic length scale used to define the Poiseuille number. Combining the above two results gives the heat transfer rate in terms of the fundamental flow quantities

$$Q_s = \frac{\rho C_p A^2 \Delta p \mathscr{L} N(\overline{T}_s - T_i)}{\mu PLPo_{\mathscr{L}}} \tag{4}$$

Eq. (4) may be written in alternate form

$$Q_s = \underbrace{\frac{\rho C_p(\overline{T}_s - T_i)\Delta p}{\mu}}_{\text{System}} \underbrace{\frac{NA^2\mathscr{L}}{PLPo_{\mathscr{L}}}}_{\text{Geometry}} \tag{5}$$

The Poiseuille number is reported for some forty different configurations in Shah and London [7] as $fRe_{D_h} = 2Po_{D_h}$, where D_h is the hydraulic diameter defined as $D_h = 4A/P$. Po_{D_h} is a numerical constant which varies with shape. Most geometric shapes have $6 < Po_{D_h} < 12$.

The value of N for a given array must be determined for the cross-section, HW, in terms of a characteristic dimension of the duct or channel in the array. Considering that $N \sim HW/\ell^2$, where ℓ is the reference length scale, it can easily be shown that the heat transfer rate has the following dependency:

$$Q_s \sim C_1 \ell^2 \tag{6}$$

when A, P, and $\mathscr{L}$ are known in terms of ℓ. For example for parallel plates this would give $\ell \sim b$, the plate spacing.

However, as we will see shortly, in the present derivation N appears in both asymptotic limits and thus cancels, and as such does not affect the outcome of the optimization. It will be shown that the solution is valid for the case of a single channel or an array of similar sized channels. The array is then constructed from these basic unit cells.

2.2. Large ducts or channels

In the case of an array of non-circular ducts or channels with large cross-sectional characteristic length scale, the heat transfer rate may be adequately approximated as boundary layer flow in this limit, Muzychka and Yovanovich [8]. The heat transfer rate is determined from

$$Q_l = \overline{h} NPL(\overline{T}_s - T_i) \tag{7}$$

where $\overline{h}$ may be defined from the expression for laminar boundary layer flow over a flat plate

$$\frac{\overline{h}L}{k_f} = 0.664\left(\frac{U_\infty L}{\nu}\right)^{1/2} Pr^{1/3} \tag{8}$$

The free stream velocity U_∞, is obtained from a force balance on the array

$$\overline{\tau}_w PLN = NA\Delta p \tag{9}$$

where the mean wall shear stress is obtained from the boundary layer solution

$$\frac{\overline{\tau}_w}{\frac{1}{2}\rho U_\infty^2} = 1.328\left(\frac{U_\infty L}{\nu}\right)^{-1/2} \tag{10}$$

Combining Eqs. (9) and (10) gives the following result for U_∞:

$$U_\infty = 1.314\left(\frac{\Delta pA}{PL^{1/2}\rho^{1/2}\nu^{1/2}}\right)^{2/3} \tag{11}$$

Finally, combining Eqs. (7), (8) and (11) yields the following result for the heat transfer rate

$$Q_l = 0.7611 N k_f(\overline{T}_s - T_i)\left(\frac{\Delta p A P^2 L Pr}{\rho \nu^2}\right)^{1/3} \tag{12}$$

We may write Eq. (12) in an alternate form

$$Q_1 = 0.7611 \underbrace{\frac{k_f(\overline{T}_s - T_i)\Delta p^{1/3} Pr^{1/3}}{\rho^{1/3}\nu^{2/3}}}_{\text{System}} \underbrace{N\left(AP^2L\right)^{1/3}}_{\text{Geometry}} \tag{13}$$

Once again, we see that the heat transfer rate is directly proportional to the number of ducts or channels in the array. Considering that $N \sim HW/\ell^2$, where ℓ is the reference length scale of the cross-section, it can easily be shown that the heat transfer rate has the following dependency:

$$Q_1 \sim C_2 \ell^{-2/3} \tag{14}$$

2.3. Optimal duct or channel size

The optimal duct or channel size may be found by means of the method of intersecting asymptotes [9,10]. The exact shape of the heat transfer rate curve may be found using more exact methods such as expressions found in Shah and London [7] for individual geometries. As shown in Fig. 2, the curves should be somewhat dependent on the duct shape. However, the intersection point of the two asymptotic results is relatively close to the exact point. In this way, an approximate value for the reference duct dimension may be found. Intersecting Eqs. (5) and (13) gives

$$0.7611 \frac{k_f(\overline{T}_s - T_i)\Delta p^{1/3} Pr^{1/3}}{\rho^{1/3}\nu^{2/3}} N\left(AP^2L\right)^{1/3} \approx \frac{\rho C_p(\overline{T}_s - T_i)\Delta p}{\mu} \frac{NA^2\mathscr{L}}{PLPo_{\mathscr{L}}} \tag{15}$$

Since N, appears on both sides of the equation, we can conclude that the optimal duct size is determined as a result of the length constraint and the pressure drop constraint and not that of the array. In other words, each optimal duct geometry represents a basic constructional element for the array, such that the array is also optimal.

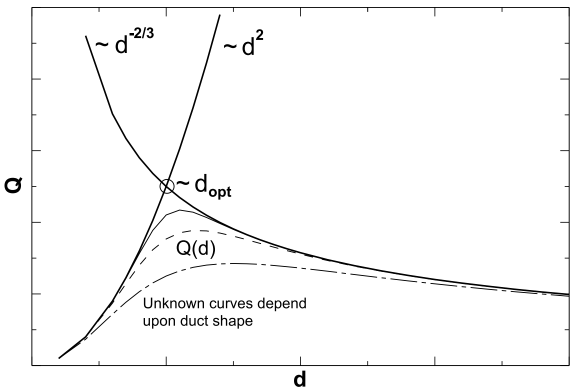

Fig. 2. Method of intersecting asymptotes.

After simplifying and collecting the system and geometry terms, the above equation may be written in the following form:

$$Be^{1/4} \approx \frac{0.9027L}{\left(\frac{A}{P}\right)^{5/8}\left(\frac{\mathscr{L}}{Po_{\mathscr{L}}}\right)^{3/8}} \tag{16}$$

where $Be = \Delta pL^2/\mu\alpha$ is the Bejan number as defined in [2,3]. The right hand side is only a function of the duct shape and aspect ratio, while the left hand side is a system parameter which is constant and independent of duct shape or aspect ratio once a cooling volume, $V = HWL$, is specified. When the hydraulic diameter is chosen, $\mathscr{L} = 4A/P$, the optimal solution is determined by solving

$$Be^{1/4} \approx 0.5365 \frac{PL}{A} Po_{D_h}^{3/8} \tag{17}$$

This result can now be applied to several fundamental shapes that are often used in convection cooling of finite volumes. Later, we will re-examine Eq. (16) using an approximate universal value for $Po_{\sqrt{A}}$ when $\mathscr{L} = \sqrt{A}$. This form allows for all of the shapes to be considered to be modeled with a single expression. Finally, all of the results in the present work are applicable for laminar flows or in terms of the Bejan number, the range defined [1] by

$$Be^{1/4} \lesssim 10^3 Pr^{1/2} \tag{18}$$

2.4. Maximum heat dissipation

The maximum heat transfer rate for a fixed volume can be obtained from Eq. (5) using the optimal result determined by Eq. (17). The number of ducts or channels N, which appears in the final result may then be cast in terms of the cooling volume cross-section HW. In this way, the maximum heat transfer per unit volume may be determined. Subsequent results may then be presented in terms of the following dimensionless heat transfer per unit volume:

$$Q^\star \lesssim \frac{\mathscr{Q}L^2}{k(\overline{T}_s - T_i)} = C_3 Be^{1/2} \tag{19}$$

where $\mathscr{Q} = Q/(HWL)$ is the heat transfer per unit volume, and C_3 is a numerical constant determined from the duct geometry.

3. Elemental geometries

We may now consider several common geometries which are convenient in electronics cooling and compact heat exchanger design. These include arrays of parallel plates, circular tubes, rectangular channels, elliptic ducts, polygonal ducts, and triangular ducts, as shown in Fig. 3.

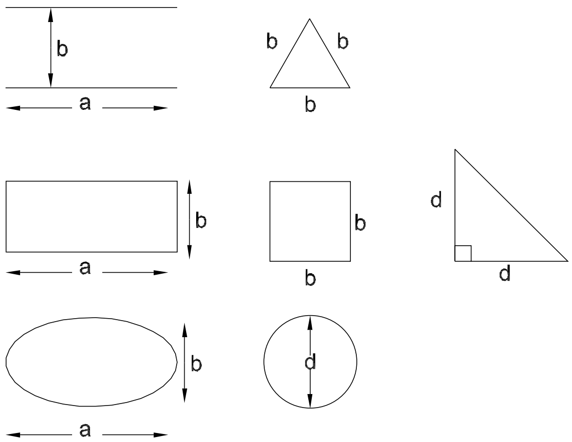

Fig. 3. Elemental geometries being considered.

3.1. Parallel plates

The problem of a finite volume cooled by a stack of parallel plates (or channels) was first considered by Bejan and Sciubba [1]. The following geometric parameters are required in the general analysis:

$$A = ab \tag{20}$$

$$P = 2a \tag{21}$$

$$D_h = 2b \tag{22}$$

$$Po_{D_h} = 12 \tag{23}$$

Substituting the above results into Eq. (17) gives the following results for the optimal plate spacing:

$$\frac{b_{opt}}{L} \approx 2.726 Be^{-1/4} \tag{24}$$

The maximum heat transfer rate for $N \sim H/b$ channels is

$$Q^\star \lesssim 0.6192 Be^{1/2} \tag{25}$$

The above results are precisely the same as those obtained by Bejan and Sciubba [1] which are also reported in Bejan [9,10].

3.2. Circular tubes

If circular tubes are used to form an array of internal flow channels, the following geometric parameters are required:

$$A = \pi d^2/4 \tag{26}$$

$$P = \pi d \tag{27}$$

$$D_h = d \tag{28}$$

$$Po_{D_h} = 8 \tag{29}$$

Substituting the above results into Eq. (17) gives the following results for the optimal tube diameter:

$$\frac{d_{opt}}{L} \approx 4.683 Be^{-1/4} \tag{30}$$

The maximum heat transfer rate for the maximum number of tubes arranged on square centers where $N \sim HW/d^2$, is

$$Q^\star \lesssim 0.5382 Be^{1/2} \tag{31}$$

The maximum dimensionless heat transfer is only 8.69% lower than the case for parallel plate channels. This difference can be attributed to the fact that tubes cannot fill the volume of space as efficiently as plane channels. This leads us to consider other geometries which allow for more efficient packing arrangements such as rectangular ducts and triangular ducts.

3.3. Rectangular ducts

In the case of an array of rectangular ducts having major axis a and minor axis b, the necessary geometric parameters are

$$A = ab \tag{32}$$

$$P = 2a + 2b \tag{33}$$

$$D_h = 2ab/(a+b) \tag{34}$$

$$Po_{D_h} = \frac{12}{(1+\epsilon)^2\left[1 - \frac{192\epsilon}{\pi^5}\tanh\left(\frac{\pi}{2\epsilon}\right)\right]} \tag{35}$$

where the duct aspect ratio is defined as $\epsilon = b/a$. Eq. (35) represents a single term approximation for the Poiseuille number with a maximum error of 0.5%, which occurs for the limit $\epsilon = 1$. Combining the above equations in Eq. (17), leads to

$$\frac{b_{opt}}{L} \approx \frac{1.0735(1+\epsilon)Po_{D_h}^{3/8}}{Be^{1/4}} \tag{36}$$

for the optimal minor axis dimension.

The maximum heat transfer rate using $N \sim HW/ab$ is

$$Q^\star \lesssim \frac{1.152 Be^{1/2}}{Po_{D_h}^{1/4}} \tag{37}$$

The following limits are obtained from the above equation:

$$\begin{aligned} Q^\star &\lesssim 0.6192 Be^{1/2}, \quad \epsilon \to 0 \\ Q^\star &\lesssim 0.7068 Be^{1/2}, \quad \epsilon \to 1 \end{aligned} \tag{38}$$

The results for b_{opt}/L and $Q^\star$ are tabulated in Table 1 as a function of ϵ. It is clear that aspect ratio has only a small effect on the maximum heat transfer rate and that there is no optimal value.

Table 1
Results for the rectangular duct

$\epsilon = b/a$	Po_{D_h}	$(b_{opt}/L)Be^{1/4}$	$Q^\star/Be^{1/2}$
0.01	11.84	2.739	0.6213
0.10	10.58	2.860	0.6390
0.20	9.54	3.000	0.6559
0.30	8.76	3.147	0.6701
0.40	8.19	3.304	0.6816
0.50	7.78	3.472	0.6905
0.60	7.49	3.651	0.6971
0.70	7.31	3.841	0.7016
0.80	7.19	4.042	0.7046
0.90	7.13	4.252	0.7062
1.00	7.12	4.470	0.7068

Table 2
Results for the elliptic duct

$\epsilon = b/a$	Po_{D_h}	$(b_{opt}/L)Be^{1/4}$	$Q^\star/Be^{1/2}$
0.01	9.87	3.226	0.5106
0.10	9.65	3.250	0.5134
0.20	9.30	3.314	0.5183
0.30	8.95	3.409	0.5233
0.40	8.65	3.532	0.5278
0.50	8.41	3.679	0.5314
0.60	8.24	3.847	0.5342
0.70	8.12	4.034	0.5361
0.80	8.05	4.237	0.5373
0.90	8.01	4.454	0.5379
1.00	8.00	4.683	0.5382

3.4. Elliptic ducts

In the case of an array of elliptic ducts having major axis a and minor axis b, the necessary geometric parameters are

$$A = \pi ab/4 \tag{39}$$

$$P = 2a\mathbf{E}(\epsilon') \tag{40}$$

$$D_h = \frac{\pi b}{2\mathbf{E}(\epsilon')} \tag{41}$$

$$Po_{D_h} = (1+\epsilon^2)\left[\frac{\pi}{\mathbf{E}(\epsilon')}\right]^2 \tag{42}$$

where $\mathbf{E}(\epsilon')$ is the complete elliptic integral of the second kind of complementary modulus $\epsilon' = \sqrt{1-\epsilon^2}$ and the duct aspect ratio is defined as $\epsilon = b/a$. Combining the above equations in Eq. (17), leads to

$$\frac{b_{opt}}{L} \approx \frac{1.367\mathbf{E}(\epsilon')Po_{D_h}^{3/8}}{Be^{1/4}} \tag{43}$$

for the optimal minor axis dimension.

The maximum heat transfer rate with $N \sim HW/ab$ is

$$Q^\star \lesssim \frac{0.9051 Be^{1/2}}{Po_{D_h}^{1/4}} \tag{44}$$

The following limits are obtained from the above equation:

$$\begin{aligned} Q^\star &\lesssim 0.5106 Be^{1/2}, \quad \epsilon \to 0 \\ Q^\star &\lesssim 0.5382 Be^{1/2}, \quad \epsilon \to 1 \end{aligned} \tag{45}$$

The results for b_{opt}/L and $Q^\star$ are tabulated in Table 2 as a function of ϵ. In the case of the elliptic duct, the range for $Q^\star$ is much smaller than that for the rectangular duct and once again there is no optimal aspect ratio.

3.5. Polygonal ducts

In the case of an array formed as a result of using polygonal ducts of side dimension b, the necessary geometric parameters are

$$A = \frac{n}{4} b^2 \cot(\pi/n) \tag{46}$$

$$P = nb \tag{47}$$

$$D_h = b\cot(\pi/n) \tag{48}$$

Also of importance are the inscribed and circumscribed diameters of a regular polygon in terms of the side dimension b

$$d_i = b\cot(\pi/n) \tag{49}$$

$$d_c = \frac{b}{\sin(\pi/n)} \tag{50}$$

These dimensions may be used to determine the nominal number of polygonal shapes that can be fit in an array if the ducts are arranged in a similar manner as circular tubes. Clearly, some shapes such as the triangle, square, and hexagon, allow for more efficient packing. We only consider one special case for maximum packing ability: the triangle, since the square has already been considered earlier.

Using the above relationships in Eq. (17), leads to the following expression for the optimal inscribed diameter which also happens to be the hydraulic diameter of a regular polygon:

$$\frac{d_{i,opt}}{L} \approx \frac{2.147 Po_{D_h}^{3/8}}{Be^{1/4}} \tag{51}$$

The Poiseuille number for regular polygons with $3 < n \leqslant 8$ is given in Table 3. Beyond $n = 8$, the Poiseuille number approaches that of the circular tube, $n = \infty$. For most practical design problems $n \leqslant 8$ suffices.

First, if we only consider packing arrangements of polygons arranged according to their circumscribed

Table 3
Results for polygonal geometries

n	Po_{D_h}	$(d_{i,\mathrm{opt}}/L)Be^{1/4}$	$Q^\star/Be^{1/2}$
3	20/3	4.373	0.2329
4	7.114	4.481	0.3528
5	7.369	4.541	0.4157
6	7.527	4.577	0.4519
7	7.655	4.606	0.4740
8	7.706	4.617	0.4891
∞	8	4.683	0.5382

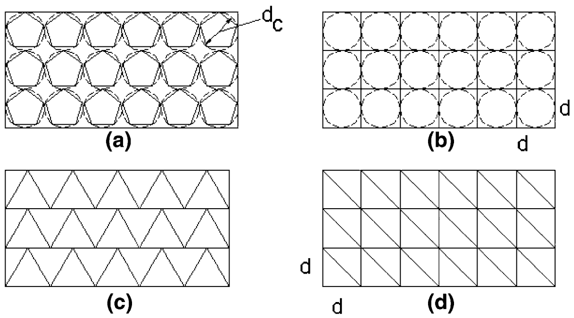

Fig. 4. Some possible packing arrangements: (a) Circumscribed polygons; (b) square ducts; (c) equilateral triangle; and (d) isosceles right triangle.

boundary as shown in Fig. 4(a), such that $N \sim HW/d_c^2$, then the maximum heat transfer rate can be shown to be

$$Q^\star \lesssim \frac{0.1440n\sin(2\pi/n)Be^{1/2}}{Po_{D_h}^{1/4}} \tag{52}$$

This equation approaches the solution for the tube in the limit of $n \to \infty$. For all values of n, the packing is not very efficient. Results are summarized in Table 3.

On the other hand, if we consider the special arrangement that a triangular duct may have (as shown in Fig. 4(c)) where $N \sim 2\sqrt{2}HW/(\sqrt{3}b^2)$, then the maximum heat transfer rate can be shown to be

$$Q^\star \lesssim 0.7172Be^{1/2} \tag{53}$$

which is comparable to the square channel shown in Fig. 4(b).

3.6. Isosceles triangular ducts

Finally, we may also examine isosceles triangular ducts in general, but only the special case of an isosceles right triangle is considered, refer to Fig 4(d). The isosceles right triangle is particularly useful since it can be uniformly packed into two arrangements of 2 or 4 elements in a square packing arrangement. The geometric characteristics of an isosceles right triangle of leg d are

$$A = \frac{1}{2}d^2 \tag{54}$$

$$P = (2+\sqrt{2})d \tag{55}$$

$$D_h = \frac{2d}{(2+\sqrt{2})} \tag{56}$$

$$Po_{D_h} = 6.577 \tag{57}$$

Using the above relationships and Eq. (17) we may determine the optimal leg dimension of the isosceles right triangle to be

$$\frac{d_{\mathrm{opt}}}{L} \approx \frac{7.428}{Be^{1/4}} \tag{58}$$

Finally, the heat transfer rate for two or four element packing arrangement such that $N \sim 2HW/d^2$ is

$$Q^\star \lesssim 0.7196Be^{1/2} \tag{59}$$

This result is the largest value of the dimensionless heat transfer per unit volume providing 1.8% greater heat transfer than the square cell. However, since we are not dealing with exact solutions, this marginal increase is likely not realizable in practice. But that is not to say that this is not a useful shape. In many compact heat exchangers triangular passages are formed through rolled fin processes as are square channel arrangements. Therefore, both shapes are the likely candidates for heat sink or heat exchanger designs containing small channels.

3.7. Arbitrary shaped ducts

Eq. (16) can be generalized further such that particular values of $Po_{\mathscr{L}}$ are not required. Muzychka and Yovanovich [11,12] showed that the Poiseuille number is a weak function of duct shape and can be predicted within 10% for most duct shapes as a function of aspect ratio only, when the characteristic length scale is $\mathscr{L} = \sqrt{A}$. The expression for the rectangular duct has been proposed as a general model [11]

$$Po_{\sqrt{A}} = \frac{6}{\sqrt{\epsilon}(1+\epsilon)\left[1 - \frac{192\epsilon}{\pi^5}\tanh\left(\frac{\pi}{2\epsilon}\right)\right]} \tag{60}$$

The above equation predicts the Poiseuille number for the shapes considered within 7.5%. Eq. (16) may now be written in the form

$$Be^{1/4} = \frac{0.9027LPo_{\sqrt{A}}^{3/8}}{(A/P)^{5/8}A^{3/16}} \tag{61}$$

after the inclusion of $\mathscr{L} = \sqrt{A}$. Since the Poiseuille number appears to the 3/8 power, the small error introduced by the approximation of the Poiseuille number with Eq. (60) becomes even smaller. The maximum error in using Eq. (61) is approximately 2.5% when compared with the results reported earlier.

4. Discussion

Several new approximate solutions for the optimal duct geometry have been obtained using the simple approach of Bejan and Sciubba [1]. For the most common and useful shapes examined, we see that arrays of square channels and equilateral or isosceles right triangles appear to yield maximum heat transfer per unit volume. The differences in these three shapes is small. On the basis of most efficient packing, the square and isosceles right triangles appear to be superior. Intuition would tend to agree with these results, as polygonal type shapes have the lowest Poiseuille numbers and hence lower flow resistance, while at the same time, these duct shapes can also provide for a large surface area per unit volume. Whereas parallel plates have the highest Poiseuille number and do not provide the ability for maximum heat transfer surface *if* they have the same spacing as a square duct. However, a quick review of the results show that the optimal duct size for a square duct is nominally larger than that of the parallel plates for the same Bejan number. Thus more surface could conceivably be packed into a fixed volume with parallel plates spaced closer together. Further, due to the nature of the approximate method, no absolute conclusion can be made as to which system is better, square duct or parallel plates? In any case, to answer these questions, one must examine more exact results using appropriate heat transfer and friction models for each shape.

5. Comparisons with more exact solutions

We now examine the accuracy of the solutions obtained using the order of magnitude approach by comparing these predictions with more exact results obtained from [1,4], for the parallel plate channel, circular duct, square duct, and triangular duct. The optimal solutions to the parallel plate configuration [1] were obtained using correlations for fluid friction and heat transfer which may be found in Shah and Sekulic [13] or Shah and London [7]. In the case of the triangular, square, and circular ducts, the correlations were generalized formulations developed by one of the authors of reference [4].

The results from Yilmaz et al. [4] were not presented in terms of the Bejan number and required conversion to the notation used in the present work. Further, the results for heat transfer were only presented for a single duct, not an array of ducts. The results for both heat transfer and optimal duct diameter have been converted to the present notation and are summarized in Tables 4 and 5. The mean values of the results presented in Table 4 for the optimal duct diameter are in excellent agreement with the approximate method presented earlier. The approximate results are 8.3%, 8.2%, and 10.8% lower than the more exact and rigorous analysis.

The results of Bejan and Sciubba [1] are also presented for completeness in Table 6. In the case of the optimal plate spacing, the exact predictions are approximately 11.7% higher than the simple approach. In all cases, the agreement between the approximate maximum heat transfer rate and the exact value increases with Prandtl number as shown in Tables 5 and 6. Two points need to be highlighted regarding the approximate method. First, the order of magnitude is correctly predicted for both parameters. Second, as discussed by Bejan and Sciubba [1], since the optimal duct dimension prediction has acceptable accuracy, one may then use conventional methods to calculate the heat transfer rate using the predicted geometry. Finally, although the order of magnitude method predicted that the square and triangular ducts had higher heat transfer per unit volume, the exact solutions clearly show that the parallel plate channel is the superior performer with approximately 10–15% greater performance depending on Prandtl number. This contradiction in results is due to the nature of the method of asymptotes. In these cases the actual heat transfer curve is lower for the square, while the intersection point of the asymptotes is higher for

Table 4
Exact values of $(d_{i,\mathrm{opt}}/L)Be^{1/4}$ for polygons versus Prandtl number [4]

Pr	Triangle	Square	Circular
0.1	4.946	5.000	5.261
1	4.515	4.635	4.971
10	4.748	4.822	5.234
100	4.728	4.885	5.284
Mean	4.734	4.836	5.188

Table 5
Exact values of $Q^{\star}/Be^{1/2}$ for polygons versus Prandtl number [4]

Pr	Triangle	Square	Circular
0.1	0.2769	0.2687	0.2348
1	0.3972	0.4127	0.3369
10	0.4499	0.4647	0.3783
100	0.4568	0.4723	0.3843

Table 6
Exact values for parallel plates versus Prandtl number [1]

Pr	$(b_{\mathrm{opt}}/L)Be^{1/4}$	$Q^{\star}/Be^{1/2}$
0.72	3.033	0.479
6	3.077	0.522
20	3.078	0.527
100	3.055	0.526
1000	3.025	0.523

the square, when compared with the parallel plate geometry.

6. Summary and conclusions

Heat transfer from arrays of microchannels was considered for fixed volume and fixed pressure drop constraints. Order of magnitude relationships were developed for the optimal reference dimension of a number of fundamental duct shapes including the rectangle, ellipse, and regular polygons. An approximate expression for the optimal duct shape was developed for all ducts considered. Comparison of the approximate results with exact results from the literature show excellent agreement for the optimal duct dimensions. Maximum dimensionless heat transfer per unit volume also agreed well with exact results, however, more accurate results should be computed using conventional methods once the optimal geometry is found using the present approach. A simple general expression for optimal duct shape was developed.

Acknowledgements

The author acknowledges the support of the Natural Sciences and Engineering Research Council of Canada (NSERC) for support provided through the Discovery Grants program. The author also acknowledges the assistance of Ms. Kelly Boone for preparation of the figures.

References

[1] A. Bejan, E. Sciubba, The optimal spacing of parallel plates cooled by forced convection, Int. J. Heat Mass Transfer 35 (1992) 3259–3264.

[2] S. Bhattacharjee, W.L. Grosshandler, The formation of a wall jet near a high temperature wall under microgravity environment, ASME HTD 96 (1988) 711–716.

[3] S. Petrescu, Comments on the optimal spacing of parallel plates cooled by forced convection, Int. J. Heat Mass Transfer 37 (1994) 1283.

[4] A. Yilmaz, O. Buyukalaca, T. Yilmaz, Optimum shape and dimensions of ducts for convective heat transfer in laminar flow at constant wall temperature, Int. J. Heat Mass Transfer 43 (2000) 767–775.

[5] T.S. Fisher, K.E. Torrance, Constrained optimal duct shapes for conjugate laminar forced convection, Int. J. Heat Mass Transfer 43 (2000) 113–126.

[6] M. Favre-Marinet, S. Le Person, A. Bejan, Maximum heat transfer rate density in two dimensional minichannels and microchannels, First International Conference on Microchannels and Minichannels, 21–23 April, Rochester, NY, 2003, pp. 765–772.

[7] R.K. Shah, A.L. London, Laminar Flow Forced Convection in Ducts, Academic Press, NY, 1978, pp. 78–283.

[8] Y.S. Muzychka, M.M. Yovanovich, Laminar forced convection heat transfer in combined entrance region of non-circular ducts, J. Heat Transfer 126 (2004) 54–61.

[9] A. Bejan, Shape and Structure, from Engineering to Nature, Cambridge University Press, Cambridge, K, 2000, pp. 35–37.

[10] A. Bejan, Convection Heat Transfer, Wiley, New York, NY, 2004, pp. 136–141.

[11] Y.S. Muzychka, M.M. Yovanovich, Laminar flow friction and heat transfer in non-circular ducts—Part I Hydrodynamic problem, in: G.P. Celata, B. Thonon, A. Bontemps, S. Kandlikar (Eds.), Compact Heat Exchangers—A Festschrift on the 60th Birthday of Ramesh K. Shah, Edizioni ETS, 2002, pp. 123–130.

[12] Y.S. Muzychka, M.M. Yovanovich, Laminar flow friction and heat transfer in non-cicular ducts—Part II Thermal problem, in: G.P. Celata, B. Thonon, A. Bontemps, S. Kandlikar (Eds.), Compact Heat Exchangers—A Festschrift on the 60th Birthday of Ramesh K. Shah, Edizioni ETS, 2002, Edizioni ETS, 2002, pp. 131–139.

[13] R.K. Shah, D. Sekulic, Fundamentals of Heat Exchanger Design, Wiley, NY, 2003, pp. 473–508.